2026 IEEE/SICE International Symposium on System Integration (SII)
January 11-14, 2026. Cancún, México

Arterial Simulator with Configurable Pulse Wave Velocity for Quantitative Tracheal Endoscopic Image Measurement

Tomohiro Sueishi[1], Makoto Komura[2], and Masatoshi Ishikawa[1]

***Abstract*— In quantitative diagnosis of tracheomalacia using endoscopic examination, it is necessary to perform spatiotemporal quantification of cardiogenic oscillations on the tracheal wall that interfere with the measurement of respiratory fluctuations. Measurement accuracy and characteristics by high-speed endoscopic imaging are unclear against cardiogenic oscillations observed in tracheal endoscopic images, which are considered to include arterial pulse waves. To understand the mechanism of such cardiogenic oscillations, it is also necessary to distinguish between arterial pulse waves and cardiac tissue motion. In this paper, we propose an arterial pulse wave simulator consisting of a pulsatile pump and an ultra-flexible tube. Pulse transit time is measured by laser displacement sensors placed at two points on the tube deformed by the pulse wave. By adjusting the pressure of the liquid inside the tube, it is possible to generate specific pulse wave velocities within a certain range. Using the adjusted pulse wave velocity as a reference value, we quantitatively evaluate the measurement accuracy of pulse waves obtained by high-speed endoscopic imaging. We have experimentally evaluated the quality of pulse wave velocity adjustment of the developed simulator and demonstrated the estimation of pulse wave velocity by endoscopic texture tracking.**

I. Introduction

Tracheomalacia [1], a condition observed in children, is characterized by symptoms such as tracheal collapse during inspiration due to weakened tracheal cartilage. Malacia is defined as a reduction of 50% or more in the expiratory cross-sectional luminal area during quiet respiration, but there is no universally agreed-upon diagnostic examination. Flexible bronchoscopy is commonly used due to no radiation exposure and short examination time, but it faces challenges related to the qualitative nature of the examination [1]. Therefore, quantification of tracheal malacia through endoscopic diagnosis is necessary to achieve equitable healthcare.

Three-dimensional measurement and modeling approaches are effective for quantitative diagnosis using endoscopy. Three-dimensional modeling of the trachea [2] reveals complex relationships between the length and location of malacia, tracheal diameter, and tissue type, and also indicates a risk of sudden airway collapse due to snap through instability. In contrast, cardiogenic oscillations can be observed in tracheal endoscopic images, and the authors have experimentally confirmed this in rabbits [3]. However, to the authors' knowledge, the quantitative spatiotemporal characteristics of such cardiogenic oscillations have not been reported. A report exists suggesting that cardiogenic oscillations degrade esophageal pressure signals and complicate analysis [4], indicating that adequate spatial quantification of tracheal cardiogenic oscillations is necessary.

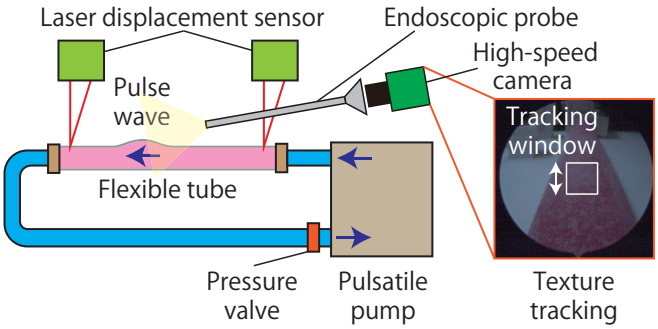

Fig. 1. A concept of the proposed arterial pulse wave simulator.

Tracheal cardiogenic oscillations are thought to include both arterial waves around the trachea and cardiac tissue motion, though their respective contributions remain unclear. The former has been extensively studied through various investigations, such as pulse wave velocity (PWV) and pulse transit time (PTT) [5]. For rabbits, commonly used in animal experiments, PWV has been reported to be around 5 m/s [6], [7]. Simulations using rabbit blood flow models estimate the PWV in arteries near the trachea to be around 10 m/s [8]. While the precision assurance of PTT measurement devices is important [9], the detailed performance of the PTT measurement system using a high-speed camera inserted into the trachea [3] has not been evaluated.

Therefore, this paper proposes an arterial pulse wave simulator using a pulsatile pump and an ultra-flexible tube to quantify the accuracy of pulse wave measurement via high-speed endoscopic imaging, with its concept shown in Fig. 1. Unlike pulse wave simulators using elastic tubes such as silicone [10], [11], [12], this simulator utilizes the ultra-flexible tube where deformation due to pulse waves is visually observable. Furthermore, to avoid inhibiting the tube deformation, we employ non-contact two-point measurement using laser displacement sensors instead of contact-based methods (e.g., linear variable differential transformer (LVDT) sensors [10]) to accurately measure PTT. Furthermore, adjusting the liquid pressure with a valve in the flow path enables configuration of the PWV. Using this adjusted PWV as a reference, we evaluate the measurement accuracy of PTT via endoscopic imaging and texture tracking using a 500 fps high-speed camera [3].

[1]T. Sueishi and M. Ishikawa are with Research Institute for Science and Technology, Tokyo University of Science, Niijuku 6-3-1, Katsushika-ku, Tokyo 125-8585, Japan. sueishi@ishikawa-vision.org
[2]Makoto Komura is with Graduate School of Medicine, The University of Tokyo, Hongo 7-3-1, Bunkyo-ku, Tokyo, 113-8656, Japan. komura-tky@g.ecc.u-tokyo.ac.jp

978-1-6654-5784-2/26/$31.00 ©2026 IEEE

II. Related Works

Fuiano et al. reviewed arterial simulator research, noting that its purpose is to elucidate complex hemodynamic phenomena and obtain meaningful parameters for cardiovascular function assessment [13]. They pointed out that systematic research is lacking regarding the effects simulators impose on the physical quantities being measured and the detailed metrological characterization of their components. Furthermore, they cite challenges with contact sensors, including insertion errors, operating environment effects (impact from water and chemicals), and difficulty mounting them on flexible tubes. They also note the frequent adoption of non-contact sensors like particle image velocimetry using cameras and laser doppler velocimetry. They conclude that challenges include issues stemming from measurement protocols, the difficulty in obtaining variations in mechanical quantities such as inner diameter, wall thickness, and Young's modulus, and discrepancies between numerical simulations and experimental results due to inadequate evaluation of boundary conditions.

Additionally, Fuiano et al. developed and validated an experimental apparatus for measuring PTT in elastic tubes using LVDT sensors [10]. They confirmed that PTT in tubes under different transmural pressure conditions are consistent with mathematical models and other research. However, they also mention the impact of inertia from the contact-type LVDT sensors on peak detection errors.

Guo et al. designed a hemodynamic pulse wave simulator for calibrating local PWV measurements [11]. They created a calibration model for cuffless blood pressure monitors using multiple linear regression on a theoretical model described by the Moens-Korteweg (MK) equation [14], as expressed in Eq. (1).

$$v_{pw} = \sqrt{\frac{Eh}{D\rho}} \tag{1}$$

v_{pw} is PWV, E is elastic modulus, D is tube diameter, h is tube wall thickness, and ρ is blood density. They simulated blood vessels using elastic tubes made of silicone rubber and measured PTT using pressure sensors. Based on the theoretical model, they experimentally demonstrated that increasing liquid pressure also increases PWV.

Unlike the MK equation [14], Ma et al. demonstrated that PWV strongly depends on pressure using a hymodynamic simulator composed of an elastic tube made of polydimethylsiloxane (PDMS) [12]. Furthermore, in human arteries, it has been shown that within the human blood pressure range, the relationship can be described by the simple formula $P = \alpha v_{pw}^2 + \beta$ (where P is pressure, and α, β are constants), and that PWV increases as blood pressure rises.

Spronck et al. summarize recommendations for validating PWV measurement devices [9]. They also note that detecting the diastolic foot (rise onset time) for PTT measurement requires a minimum sampling frequency of 120 Hz, and recommend a time resolution of 1 ms, for example, to minimize quantization error. They also mention that for verifying devices based on new principles or different arterial segments, algorithms and conversion formulas should be disclosed, and it should be clearly stated that the values provided are estimates.

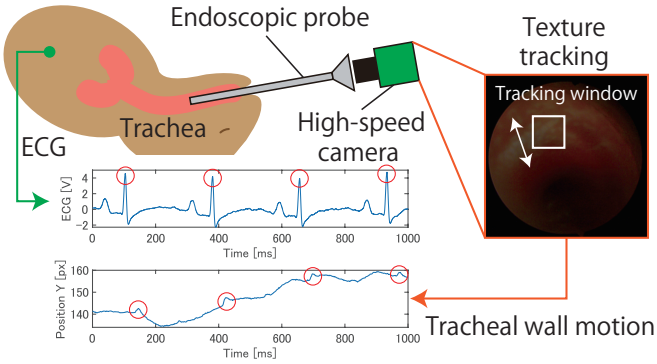

Fig. 2. Tracheal endoscopic image measurement [3].

III. Tracheal Endoscopic Image Measurement

Before describing the proposed arterial pulse wave simulator, we explain the high-speed endoscopic imaging system [3] to be evaluated. The system overview and an example of measured waveforms are shown in Fig. 2. This waveform data was measured using a New Zealand White rabbit in an experiment approved by the animal experiment committee at the University of Tokyo (A2023M138).

This system synchronously measures high-speed camera images (500 fps) and electrocardiogram (ECG) signals. For the recorded images, correlation image processing (MOSSE [15]) is used to track specific texture regions (window-based) and measure the movement of the tracheal wall. Since minute movements of the tracheal wall are observed immediately after the R wave in the synchronized ECG, it is inferred that cardiac or arterial fluctuations affect the trachea. This cardiogenic oscillations could become a challenge for quantitative endoscopic diagnosis for tracheomalacia [1]. Furthermore, it would be desirable to analyze whether it possesses characteristics such as pulse waves.

IV. Proposed Arterial Simulator

A. System Configuration

The system configuration of the proposed simulator is shown in Fig. 3. The liquid circulation system (water is used in this paper) employs a pulsatile pump, a tank, and a sufficiently rigid tube, and part of the flow path is replaced with a flexible tube. When the pulse wave generated by the pump flows through the circuit, this highly flexible tube undergoes visually noticeable deformation. Two laser displacement sensors are positioned at both ends of the flexible tube to non-contact measure this deformation. By comparing the measurement waveforms from these sensors, the PTT of the simulator is calculated. Furthermore, the pattern on the surface of the flexible tube with the deformation, enables texture tracking image processing [3], [15] in endoscopic imaging.

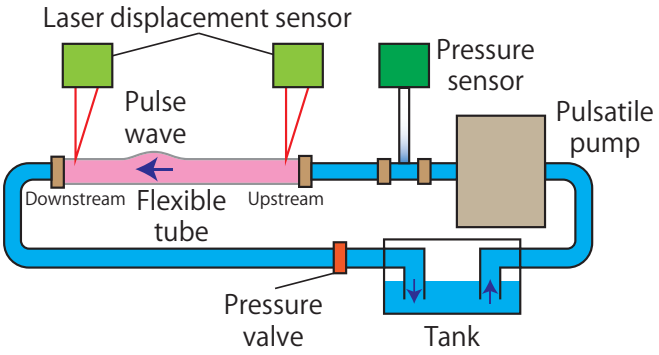

Fig. 3. Simulator system configuration.

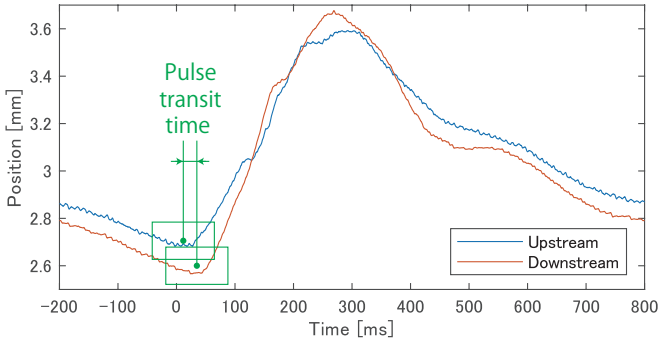

Fig. 4. Pulse waves measured by laser displacement sensors and PTT estimation.

Additionally, water pressure is adjusted by opening and closing the pressure valve at the point where water returns to the tank, and this pressure is monitored using a pressure sensor near the pulsatile pump. Adjusting the water pressure not only regulates the PWV but also prevents irreversible expansion deformation or rupture of the flexible tube caused by excessive pressure. Furthermore, using only part of the flow path as flexible tubing, with the remainder as rigid tubing, minimizes the impact of such damage. Note that the tank, pressure valve, and pressure sensor are included as standard components in the commercial pulsatile pump used in this experiment.

B. Estimation of Pulse Transit Time

Here, we describe a method for estimating PTT using measured waveforms from two locations obtained with laser displacement sensors. Examples of two waveforms are shown in Fig. 4. Note that a Savitzky-Golay filter [16] has been applied to these waveforms to reduce noise. While some studies [10] use the difference in peak times for PTT calculation, the difference in foot times, which is less susceptible to reflected waves, is commonly used [17]. Indeed, in Fig. 4, the upstream peak waveform is not sharp. Additionally, a staircase-like waveform is observed around 120 ms upstream and around 180 ms downstream. This is thought to be due to changes in the flow path at the connector linking the tubes [18], and avoiding such situations is difficult in flexible tubing where rupture is possible. Therefore, this paper employs wave foot estimation [17] for estimating PTT.

PWV is calculated by dividing the known distance (i.e., the distance between the two laser displacement sensors) by the PTT. Regarding the estimation of the time of arrival of the wave foot, it has been reported that significant differences in PWV occur depending on the estimation methods [17]. Instead of methods based on differentiation or tangents, this paper employs a diastole-patching method proposed in [17] to estimate the wave foot. This technique draws inspiration from patching in image processing algorithms, calculating the time point where the error between the patch and the distal waveform is minimized. For simplicity, this paper manually sets the patch range. The wave height is normalized (scaled to the range 0 to 1) before and after the pulse wave, and the offset value minimizing the positional difference (vertical direction in Fig. 4) is determined using a least squares method (a Levenberg-Marquardt algorithm [19]). The time offset value (i.e., the PTT from foot to foot) that minimizes the residuals in the least squares method is found through exhaustive search.

C. Configuration of Pulse Wave Velocity

PWV is a medically important parameter shown to correlate with arterial stiffness. Regarding the clinical significance of measurement error, it has been noted that a difference of approximately 0.5 m/s in PWV corresponds to a 7.5% increase in cardiovascular mortality risk [17]. For arterial simulators aimed at evaluating measurement accuracy [9], it is desirable that the PWV be adjustable, especially when compared to PWVs where the speed is known to some extent (5–10 m/s in rabbits [6], [7], [8]). Adjustable PWV can be useful not only for verifying the accuracy of medical devices but also for simulations prior to diagnosis or treatment by mimicking the PWV specific to each patient.

As mentioned in Sec. II, simulators using silicone or latex rubber tubing [11], [20] have reported that PWV increases with pressure (or peak pressure). On the other hand, in simulators using PDMS tubing [12], the graph (Fig. 2F in [12]) indicates that PWV decreases with increasing pressure. Therefore, this paper hypothesizes that the PWV through flexible tubes exhibiting visually significant deformation can also be similarly adjusted (increased or decreased) by pressure changes. Furthermore, it clarifies the relationship between PWV measured by laser displacement sensors and water pressure adjusted by the pressure valve, based on experimental measurement data.

V. Experimental Evaluation

A. Experimental Simulator

The experimental simulator is shown in Fig. 5. The pulsatile pump used was the Fuyo ALPHA FLOW EC-1. This pulsatile pump is equipped with terminals capable of outputting ECG pulses synchronized with the pulse flow. The pressure sensor (rated measurement range: from 0 to 720 mmHg), pressure valve, and tank were those supplied with the pulsatile pump. The measured pressure was verified as a relative value by confirming the numerical value displayed on

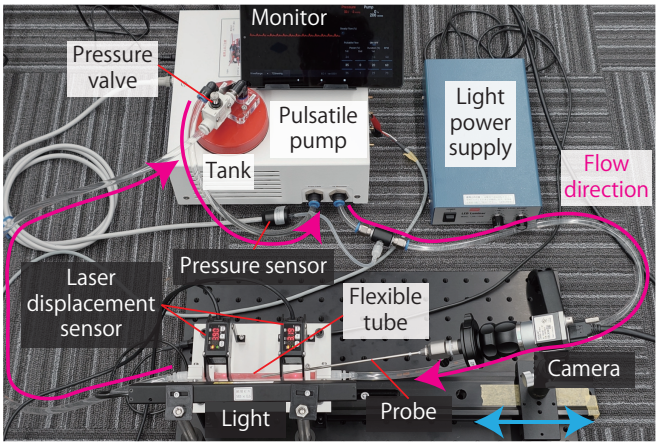

Fig. 5. Experimental system; the arterial simulator (Sec. V-B, V-C) and endoscopic imaging system (Sec. V-D).

the pulsatile pump's monitor. Three types of Hagitec ultra-flexible rubber tube (Shore A hardness 0° as a reference value) were used for the flexible tubing; HGCT-1011 (inner diameter (ID) 10 mm, outer diameter (OD) 11 mm, length 140 mm), HGCT-5060 (ID 5.0 mm, OD 6.0 mm, length 120 mm), and HGCT-3040 (ID 3.0 mm, OD 4.0 mm, length 120 mm). Urethane tubing (ID 5 mm, OD 8 mm) was used for the tubes constituting the majority of the flow path. Water was used as the liquid. To prevent the flexible tube from rupturing due to high water pressure caused by gravity, the flexible tube was positioned higher than the urethane tube's flow path.

Before adjusting the PWV, the water pressure was set using the following procedure. The flow path was filled with water, and air bubbles were removed as much as possible. Then, the relative pressure was set to 0 mmHg when the pump was not flowing. Instead of a pulse wave, a weak steady flow (11%, displayed discharge volume about 60 ml/min) was introduced. The pressure valve was opened and closed (i.e., the screw was turned) to adjust the relative pressure value to the desired level. Care was taken to avoid applying excessive pressure (e.g., relative pressure $\geq$20 mmHg) to prevent irreversible deformation or rupture of the flexible tube. A weak pulsatile flow was then introduced to measure the PTT. This pump allows setting the ratio of output power and duration between high output (corresponding to cardiac systole) and low output (corresponding to diastole). In this study, high output was set to 35%, low output to 0%, and the high output duration to 20%. The heart rate was set to 60 bpm (i.e., once per second).

Two Panasonic HG-C1050 laser displacement sensors (measuring center distance 50 mm, measuring range $\pm$15 mm, repeatability 30 μm, standard delay time 10 ms) were used. The distance between the sensors was set to 75 mm. The analog output voltage values of the laser displacement sensors and the ECG pulse voltage of the pulsatile pump were measured using a multi-channel data logger Keyence NR-500 (every 10 μs). To remove noise from the displacement signals, the Savitzky-Golay filter [16] (2nd order, 501 samples, i.e., approximately 5 ms) was applied.

B. Tube Displacement by Pulse Wave

Fig. 6 shows examples of pulse waves measured upstream and downstream at different tube diameters and relative pressure settings. For HGCT-1011, the pressure valve could not be set below 1 mmHg even when opened, so measurements were taken at 2 mmHg or higher. The rise of the ECG pulse was set as time 0 ms. In all cases, deformation due to the pulse wave of approximately 0.5 to 1 mm was confirmed. Furthermore, in the larger-diameter HGCT-1011 and HGCT-5060, expansion of approximately 1 to 1.5 mm was confirmed due to pressure increase. In the smaller-diameter HGCT-3040, an increase in the peak position due to pressure change was also confirmed.

This expansion is considered to show a larger change than that observed in various elastic tubes used in previous studies. For the PDMS tube [12] (inner diameter 12.7 mm), linearity was observed with approximately 22% expansion at 100 kPa pressure (Fig. S2 in [12]), and evaluation of PWV changes was performed around 0 to 15 kPa (Fig. 2F in [12]). Therefore, the displacement is estimated to be approximately 0.4 mm, corresponding to about a 3% diameter change. For the latex rubber tube [20] (outer diameter 22.22 mm, inner diameter 19.05 mm), expansion due to pressure change is mentioned as 0.15 mm/mmHg, but the displacement caused by the pulse wave is unknown. For a silicone rubber tube [11] (inner diameter 5 mm, wall thickness 1 mm, Shore hardness 28A), no mention is made of displacement caused by pulse waves. Another silicone tube [10] (inner diameter 25 mm, wall thickness 1.5 mm) reports a maximum change of approximately 0.28 mm. It has also been noted that approximately 1 mm of change occurs in the healthy human aorta (radius $\sim$12.5 mm) [10]. Compared to other literature, Fig. 6 can be said to reproduce displacement of the similar magnitude to the human aorta.

C. Pulse Wave Velocity Evaluation

For pulse waves under various settings including Fig. 6, the PTT estimation described in Sec. IV-B was applied. The average and standard deviation of each set of 10 computed PTTs are shown in Fig. 7, while the PWV calculated from the average PTT is shown in Fig. 8. For the diastole-patching method [17], two patch ranges were applied; (1) -30 ms to 60 ms and (2) -30 ms to 70 ms. Fig. 7 shows results for patch range (1), while Fig. 8 shows results for both patch ranges.

From Fig. 7 and Fig. 8, a decrease in PWV with increasing pressure was observed in the thick HGCT-1011, while a nonlinear relationship between PWV and pressure change was observed in HGCT-5060. This nonlinear relationship is thought to be caused, in part, by the MK equation in Eq. (1), where the increase in diameter D and decrease in wall thickness h due to the tube high flexibility contribute more significantly than the increase in elastic modulus E caused by the pulse wave. Another reason may be that the tube becomes flattened following the peak of the pulse wave.

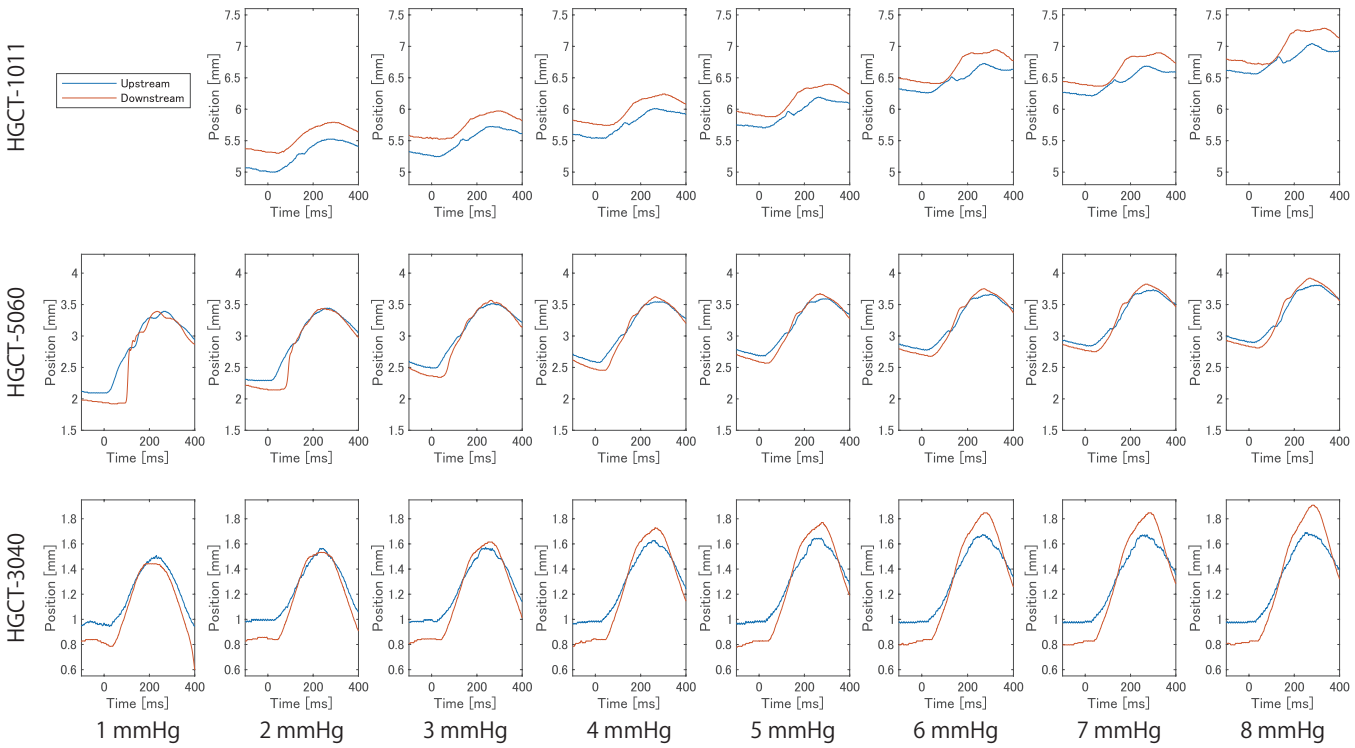

Fig. 6. Upstream and downstream pulse wave measured signals at different flexible tube diameters and relative pressures.

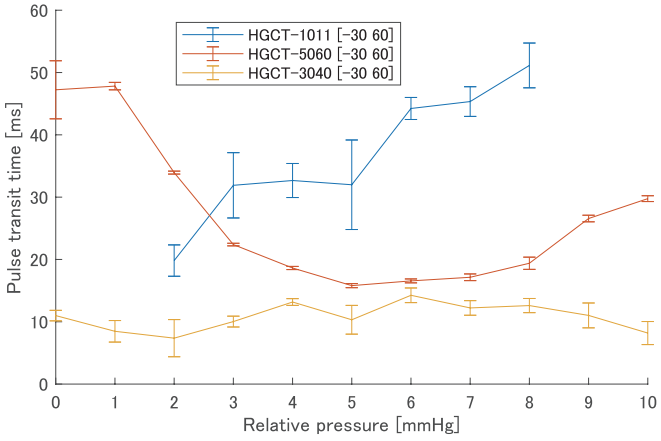

Fig. 7. Estimated PTT with laser displacement sensors.

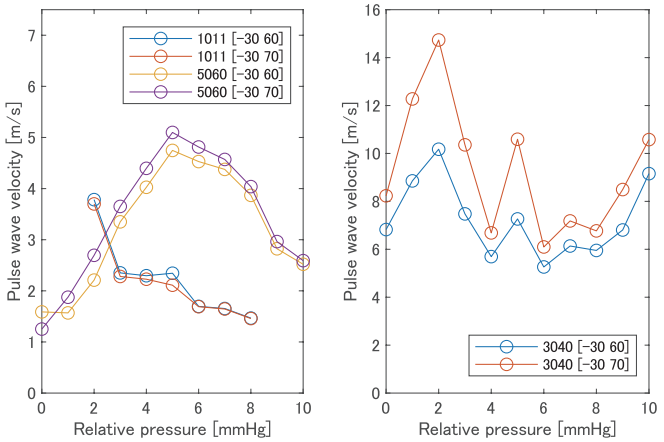

Fig. 8. Estimated PWV with laser displacement sensors.

Although a higher PWV was observed in the thinner HGCT-3040, the relationship with pressure was unclear, possibly due to insufficient measurement conditions or accuracy in the simulator.

Regarding differences in patch size, significant variations in estimated PWV were observed, particularly with the HGCT-3040. As pointed out in [17], changes in the method for estimating the wave foot can lead to considerable differences in PWV. Therefore, it is conceivable that even with the same algorithm, differences in parameters can result in variations in PWV. However, based on the results from the HGCT-5060 in particular, it is considered unlikely that these differences would significantly alter the overall upward or downward trend of the graph.

Regarding the magnitude of PWV, values close to those reported in rabbits (5 m/s [6], [7]) and simulation estimates for arteries near the trachea (10 m/s [8]) were achieved. Therefore, we judge that the measured PWV is sufficiently high for evaluating the accuracy of endoscopic imaging in animal experiments using rabbits. To stably reproduce higher PWVs, it is considered necessary to improve the reproduction accuracy for the thinner HGCT-3040, where high PWVs may occur.

D. Image Measurement Accuracy

The endoscopic imaging system evaluated using the proposed simulator is shown in the lower right of Fig. 5. A

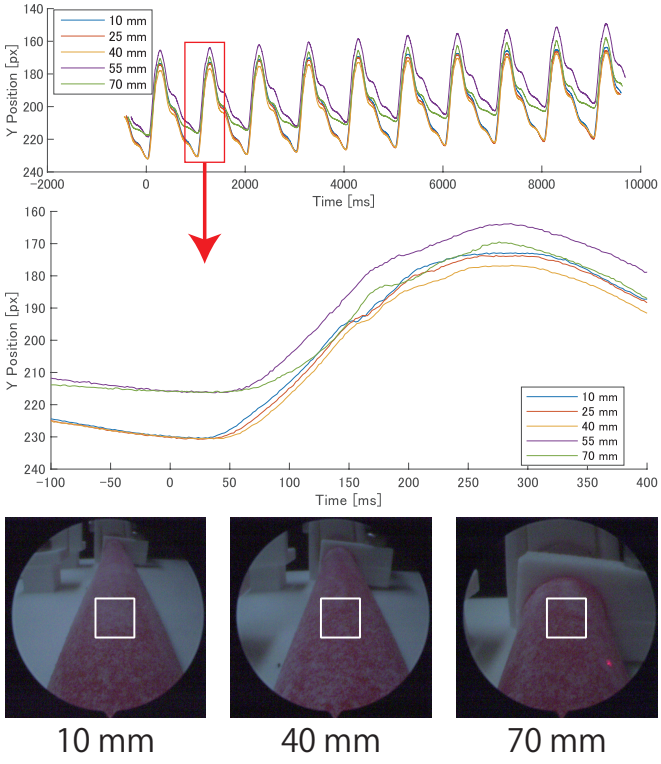

Fig. 9. Tracking window motion and sample captured images with the texture tracking window.

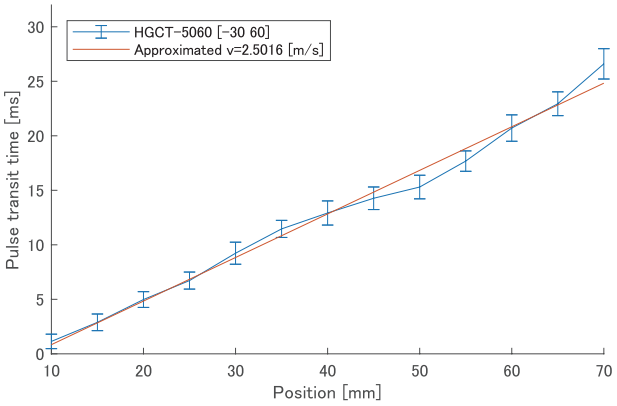

Fig. 10. Estimated PTT by image measurement.

Basler acA800-510uc (500 fps, 512×512 px) high-speed camera was used. The endoscopic probe consists of an industrial borescope (Shodensha BAL-02718, OD 2.7 mm, length 175 mm, field of view angle about 50 deg) and a variable magnification camera adapter lens (BA-A1835). For illumination, the Nissin Electronics WDL-20015 (white) and its power supply LPR-100W were used. The HGCT-5060 was selected as the measurement tube. The observation position at the end of the endoscope probe was set to be movable in 5 mm increments from the upstream area to the downstream area. Images were saved for 10 seconds (5,000 frames) at each position and analyzed offline.

Fig. 9 shows the variation in the Y-coordinate position of the window for texture tracking using MOSSE [15] and an example of captured images with the tracking window drawn. The initial window position was kept the same for each dataset. We also confirmed that waveforms similar to those measured by the laser displacement sensors could be extracted for approximately 10 seconds of tracking. However, gradual movement (i.e., drift) was observed in the position of the tracking window. This occurs because the registered texture in the correlation filter MOSSE [3], [15] is updated continuously. It is a phenomenon that is difficult to avoid in situations where prior texture registration is challenging, such as on the tracheal wall.

Furthermore, the PTT estimated from the pulse waves measured at each position is shown in Fig. 10. Using the waveform measured at the 5 mm position as a reference, the relative timing of waveforms at other positions was calculated using the diastole-patching method [17]. The patch range was set from -30 ms to 60 ms. When fitting a straight line to the average timing at each position, the slope represented the PWV, calculated to be approximately 2.5 m/s. The PWV measured by the laser displacement sensors, adjusted for pressure, ranged from 2.7 to 2.9 m/s. Therefore, it can be concluded that the values estimated by image processing are relatively close. The slight difference from the laser displacement sensors reference value is thought to be due to differences in waveform and the accuracy of calculating the wave foot.

However, when measuring PWV in the actual trachea using the high-speed endoscopic imaging [3], several challenges remain. Stabilizing the position of the endoscopic probe tip is difficult, necessitating three-dimensional position estimation of the endoscopic camera itself [21]. Furthermore, since heart and respiratory rate fluctuate in actual living organisms, it is desirable to measure at different positions at the same time rather than comparing measurement data taken at different times and different positions. That is, it is desirable to be able to measure the movement of different tracheal wall positions observed in the same image, but the distance between these different measurement positions must also be measured. Therefore, integration with dimensional measurement technologies, such as a three-dimensional measurement system [22] for endoscopic images, will also be necessary in the future.

VI. Discussion and Conclusions

This paper focuses on quantitative endoscopic diagnosis for tracheomalacia, and proposes an arterial pulse wave simulator for evaluating the measurement accuracy of high-speed endoscopic imaging. Using a flexible tube where deformation can be visually confirmed and non-contact measurement between two points with laser displacement sensors, the pulse transit time (PTT) from foot to foot can be calculated. Furthermore, through water pressure adjustment, we experimentally identified the nonlinear relationship between pressure and pulse wave velocity (PWV). This demonstrated the feasibility of setting PWVs comparable to those observed in animal experiments simulating tracheomalacia. We also

confirmed that the proposed arterial pulse wave simulator can be utilized to evaluate the measurement accuracy of PWV through positional adjustments of the high-speed endoscopic imaging system.

A limitation of the proposed method is the difficulty in handling due to the flexibility of the tube. Excessive pressure can easily cause irreversible expansion or rupture of the flexible tube, necessitating greater caution in path design and pressure control compared to conventional elastic tubes with smaller deformations. Furthermore, the relationship between pressure and PWV demonstrated in the experiments lacks sufficient theoretical interpretation. The relationship between pressure and PWV in highly deformable flexible tubes should be clarified, drawing on theoretical analyses such as [12]. This is expected to enable more stable velocity settings.

In the future, we will improve the estimation method for the rising edge of the pulse wave and the measurement accuracy of the laser displacement sensors to enable more precise calculation of PTT and PWV. Furthermore, we will conduct theoretical analysis and verification of the experimentally confirmed nonlinear relationship between pressure and PWV, aiming to build a simulator with higher reproducibility. We will then systematically improve the high-speed endoscopic imaging system, integrate it with 3D measurement, and perform more rigorous accuracy evaluation. By carefully examining the effects of differences between simulator surface and tracheal wall textures, we will clarify the feasibility of pulse wave measurement in the living trachea and lead to quantitative diagnosis of tracheomalacia.

REFERENCES

[1] Colin Wallis, Efthymia Alexopoulou, Juan L. Antón-Pacheco, Jayesh M. Bhatt, Andrew Bush, Anne B. Chang, Anne-Marie Charatsi, Courtney Coleman, Julie Depiazzi, Konstantinos Douros, Ernst Eber, Mark Everard, Ahmed Kantar, Ian B. Masters, Fabio Midulla, Raffaella Nenna, Derek Roebuck, Deborah Snijders, and Kostas Priftis. ERS statement on tracheomalacia and bronchomalacia in children. *European Respiratory Journal*, 54(3), 2019.

[2] Scott J Hollister, Maximilian P Hollister, and Sebastian K Hollister. Computational modeling of airway instability and collapse in tracheomalacia. *Respiratory Research*, 18:1–8, 2017.

[3] T Sueishi, M Komura, and M Ishikawa. High-speed image-based measurement method of tracheal cardiac-induced pulse transit time. In *The 46th Annual International Conference of the IEEE Engineering in Medicine and Biology Society (EMBC)*, 2024. Poster ID.118373.

[4] Thomas F Schuessler, Stewart B Gottfried, Peter Goldberg, Robert E Kearney, and Jason HT Bates. An adaptive filter to reduce cardiogenic oscillations on esophageal pressure signals. *Annals of Biomedical Engineering*, 26:260–267, 1998.

[5] Lukáš Peter, Norbert Noury, and M Cerny. A review of methods for non-invasive and continuous blood pressure monitoring: Pulse transit time method is promising? *IRBM*, 35(5):271–282, 2014.

[6] Shin-ichiro Katsuda, Kenji Takazawa, Masao Miyake, Daisuke Kobayashi, Masahiko Kusanagi, and Akihiro Hazama. Local pulse wave velocity directly reflects increased arterial stiffness in a restricted aortic region with progression of atherosclerotic lesions. *Hypertension Research*, 37:892–900, 2014.

[7] Leroy L. Cooper, Katja E. Odening, Min-Sig Hwang, Leonard Chaves, Lorraine Schofield, Chantel A. Taylor, Anthony S. Gemignani, Gary F. Mitchell, John R. Forder, Bum-Rak Choi, and Gideon Koren. Electromechanical and structural alterations in the aging rabbit heart and aorta. *American Journal of Physiology-Heart and Circulatory Physiology*, 302(8):H1625–H1635, 2012.

[8] Jordi Alastruey, Simon R Nagel, Bettina A Nier, Anthony AE Hunt, Peter D Weinberg, and Joaquim Peiró. Modelling pulse wave propagation in the rabbit systemic circulation to assess the effects of altered nitric oxide synthesis. *Journal of Biomechanics*, 42(13):2116–2123, 2009.

[9] Bart Spronck, Dimitrios Terentes-Printzios, Alberto P Avolio, Pierre Boutouyrie, Andrea Guala, Ana Jerončić, Stéphane Laurent, Eduardo CD Barbosa, Johannes Baulmann, Chen-Huan Chen, et al. 2024 recommendations for validation of noninvasive arterial pulse wave velocity measurement devices. *Hypertension*, 81(1):183–192, 2024.

[10] Fabio Fuiano, Giorgia Fiori, Federica Vurchio, Andrea Scorza, and Salvatore A Sciuto. Transit time measurement of a pressure wave through an elastic tube based on LVDT sensors. In *Proceedings of the 24th IMEKO TC4 International Symposium*, pages 321–326, 2020.

[11] Cheng-Yan Guo, Jau-Woei Perng, Li-Ching Chen, and Tung-Li Hsieh. A hemodynamic pulse wave simulator designed for calibration of local pulse wave velocities measurement for cuffless techniques. *Micromachines*, 14(6):1218, 2023.

[12] Yinji Ma, Jungil Choi, Aurélie Hourlier-Fargette, Yeguang Xue, Ha Uk Chung, Jong Yoon Lee, Xiufeng Wang, Zhaoqian Xie, Daeshik Kang, Heling Wang, et al. Relation between blood pressure and pulse wave velocity for human arteries. *Proceedings of the National Academy of Sciences*, 115(44):11144–11149, 2018.

[13] Fabio Fuiano, Andrea Scorza, and Salvatore Andrea Sciuto. Functional and metrological issues in arterial simulators for biomedical testing applications: A review. *Metrology*, 2(3):360–386, 2022.

[14] J Crighton Bramwell and Archibald Vivian Hill. The velocity of pulse wave in man. *Proceedings of the Royal Society of London. Series B, Containing Papers of a Biological Character*, 93(652):298–306, 1922.

[15] David S Bolme, J Ross Beveridge, Bruce A Draper, and Yui Man Lui. Visual object tracking using adaptive correlation filters. In *2010 IEEE Computer Society Conference on Computer Vision and Pattern Recognition*, pages 2544–2550, 2010.

[16] Abraham Savitzky and Marcel JE Golay. Smoothing and differentiation of data by simplified least squares procedures. *Analytical Chemistry*, 36(8):1627–1639, 1964.

[17] Orestis Vardoulis, Theodore G Papaioannou, and Nikolaos Stergiopulos. Validation of a novel and existing algorithms for the estimation of pulse transit time: advancing the accuracy in pulse wave velocity measurement. *American Journal of Physiology-Heart and Circulatory Physiology*, 304(11):H1558–H1567, 2013.

[18] Jonathan P Mynard, Avinash Kondiboyina, Remi Kowalski, Michael MH Cheung, and Joseph J Smolich. Measurement, analysis and interpretation of pressure/flow waves in blood vessels. *Frontiers in Physiology*, 11:1085, 2020.

[19] Richard Hartley and Andrew Zisserman. *Multiple view geometry in computer vision*. Cambridge University Press, 2003.

[20] Jeffrey S Lillie, Alexander S Liberson, Doran Mix, Karl Q Schwarz, Ankur Chandra, Daniel B Phillips, Steven W Day, and David A Borkholder. Pulse wave velocity prediction and compliance assessment in elastic arterial segments. *Cardiovascular engineering and technology*, 6:49–58, 2015.

[21] Takaaki Sugino, Ryoichi Nakamura, Akihito Kuboki, Osamu Honda, Masashi Yamamoto, and Nobuyoshi Ohtori. Comparative analysis of surgical processes for image-guided endoscopic sinus surgery. *International Journal of Computer Assisted Radiology and Surgery*, 14:93–104, 2019.

[22] Christoph Schmalz, Frank Forster, Anton Schick, and Elli Angelopoulou. An endoscopic 3D scanner based on structured light. *Medical Image Analysis*, 16(5):1063–1072, 2012.